Dear Dr. Michel Tsamados,

Here are the revised manuscript and the answers to your comments.

-Mean state of sea ice thickness. Be more specific on how this validation was performed, i.e. satellite data or PIOMAS.

The validation of the Arctic sea ice extent and thickness was done using satellite observation (Jahn et al., 2016;Swart et al., 2015;Barnhart et al., 2016) and also using PIOMAS (Labe et al., 2018).

- Appending procedure seems odd as one would expect a unnatural periodicity (i.e. the duration of each ensemble member run). Was this done for the historical (1920-2005) and future scenarios? Clarify the method a little bit more.

This was done for pre-industrial, historical (1920-2005) and future (2006-2050) periods. Since the sea ice thickness fields are preprocessed by removing the ensemble mean, we do not expect to see a periodicity link to the appending procedure. The appending procedure for analysing the spatial variability for all ensemble member was proposed by Referee 2 and allready used in previous works (Labe et al., 2018). The method consists of removing the ensemble mean to each member, append the SIT fields over time all together, and then apply the PCA. The method is described in the updated paper [p. 3, l. 65-71].

-Sign on new figure 1 different. Is that an error?

This is not an error, the sign of a PCA mode does not have meaning.

- Add some comments about how you expect your result to fare with other CMIP models.

This will depend on how the CESM-LE differs from the CMIP models in terms of sea ice state. The CESM-LE sea ice mean state is well validated. Both CESM-LE and CMIP5 sea ice trends over the observational period are nearly identical (Barnhart et al., 2016). So, we expect that the main mode of Arctic sea ice spatial and temporal variability of the CMIP simulated sea ice would look similar to our results.

Brief communication: Arctic sea ice thickness internal variability and its changes under historical and anthropogenic forcing

Guillian Van Achter[1], Leandro Ponsoni[1], François Massonnet[1], Thierry Fichefet[1], and Vincent Legat[2]

[1]Georges Lemaitre Center for Earth and Climate Research, Earth and Life Institute, Université Catholique de Louvain.
[2]Institute of Mechanics, Materials and Civil Engineering, Applied Mechanics and Mathematics, Université catholique de Louvain.

Correspondence: Guillian Van Achter (guillian.vanachter@uclouvain.be)

Abstract. We use model simulations from the CESM1-CAM5-BGC-LE dataset to characterise the Arctic sea ice thickness internal variability both spatially and temporally. These properties, and their stationarity, are investigated in three different contexts: (1) constant ~~,~~ pre-industrial, (2) historical and (3) projected conditions. Spatial modes of variability show highly stationary patterns regardless of the forcing and mean state. A temporal analysis reveals two peaks of significant variability and despite a non-stationarity on short ~~time-scales~~timescales, they remain more or less stable until the first half of the 21st century, where they start to change once summer ice-free events occur, after 2050.

1 Introduction

In the recent decades, Arctic sea ice has retreated and thinned significantly (Notz and Stroeve, 2016). The annual mean Arctic sea ice extent has decreased by $\sim 2 \times 10^6$ km^2 between 1979 and 2016 (Onarheim *et al.*, 2018). An analysis combining US Navy submarine ice draft measurements and satellite altimeter data showed that the annual mean sea ice thickness (SIT) over the Arctic Ocean at the end of the melt period decreased by 2 m between the pre-1990 submarine period (1958-1976) and the Cryosat-2 period (2011-2018) (Kwok, 2018). On long timescales (~~several~~ a few decades or more), ~~these retreat~~ retreating and thinning are projected to continue as greenhouse gas emissions are expected to rise. However, on shorter timescales (1-20 yr), internal climate variability, defined as the variability of the climate system that occurs in the absence of external forcing and caused by the system's chaotic nature, limits the predictability of climate (Deser *et al.*, 2014) and represents a major source of uncertainty for climate predictions (Deser *et al.*, 2012). In this context, greater knowledge of Arctic ~~sea ice thickness~~ SIT internal variability and of its drivers are both essential to document the true evolution of the Arctic atmosphere–ice–ocean system and to predict its future changes.

The mean spatial distribution of the Arctic ~~sea ice thickness~~ SIT is relatively well documented (Stroeve *et al.*, 2014). But there are some uncertainties around its interannual variability and its spatial modes of variability. Some studies (~~Singarayer and Bamber, 2003;~~ Lindsay and Zhang, 2006; Fuckar *et al.*, 2016; Labe *et al.*, 2018) already analysed the spatial distribution of Arctic sea ice variability by applying empirical orthogonal functions (EOF) (K-means cluster analysis for Fuckar *et al.*, 2016) to ~~historical sea ice thickness~~ model-based historical SIT time series. ~~They reported that the first mode is~~ Lindsay and

Zhang (2006) reported a first mode nearly basinwide, while the second and third ones are orthogonal lateral modes accounting for 30, 18 and 15% of the variability, respectively. Fuckar *et al.* (2016) also found a nearly basinwide first mode, with an Atlantic-Pacific dipole as the second mode. Labe *et al.* (2018) depicted an Atlantic-Pacific dipole but as the first mode. The spatial structure and amount of explained variance of those modes are sensitive whether and how the SIT time series is detrended. It is also model-dependent and influenced by the season and analysed period. The temporal sea ice volume (SIV) variability has been studied by Olonscheck and Notz (2017). ~~They enlightened a rather stable internal variability of annual sea ice volume and area for the historical climate compared to the~~ These authors enlightened a remarkable similarity between the pre-industrial ~~one and an extremely likely~~ and historical internal variabilities of the annual Arctic SIV. They also noticed a decreased internal variability of winter and summer Arctic ~~sea ice volume~~ SIV for a future climate forced by the RCP8.5 scenario.

~~Most of~~ Apart from Olonscheck and Notz (2017), the studies cited above used data covering a few decades under historical forcing. In this work we use a long climate model control run under pre-industrial conditions from the CESM1-CAM5-BGC-LE dataset, which enables us to study only the internal variability of the Arctic ~~sea ice thickness~~SIT. We study the internal variability both temporally and spatially by applying a wavelet analysis and an EOF decomposition to the ~~Arctic sea ice volume and thickness~~ pan-Arctic SIV and gridded SIT anomaly time series, respectively. We also determine whether or not the ~~sea ice volume and thickness~~ SIV and SIT variability is stationary by analysing the model outputs under historical and future climate conditions with 30 ensemble members.

This manuscript is organised as follows. The model and its outputs are briefly described in Section 2. In Section 3, the spatial and temporal internal variability of Arctic sea ice are analysed, as well as their persistence through historical and future climate conditions. Then we explore the drivers of the main modes of internal variability. Conclusions are finally given in Section 4.

2 Data and methods

2.1 Sea ice thickness and volume datasets

We use the CESM1-CAM5-BGC-LE dataset (Kay *et al.*, 2015). The Community Earth System Model Large Ensemble (CESM-LE) was designed to both disentangle model errors from internal climate variability and enable the assessment of recent past and future climate changes in the presence of internal climate variability. The CESM1(CAM5) ~~model~~ is a CMIP5 participating-model. It consists of coupled atmosphere, ocean, land and sea ice component models. It also includes a representation of the land carbon cycle, diagnostic biogeochemistry calculations for the ocean ecosystem and a model of the atmospheric carbon dioxide cycle (Moore *et al.*, 2013; Lindsay *et al.*, 2014). While it is not possible to validate the data in terms of SIT and SIV variabilities due to the lack of continuous observational data, the model was well validated in terms of mean state of the ice thickness and extent, as well as regarding the recent trends in the latter. Jahn *et al.* (2016) showed good agreement between observations and CESM1(CAM5) simulations for mean Arctic sea ice thickness and extent in the early twenty-first century~~, and~~ . Barnhart *et al.* (2016) demonstrated that CESM1(CAM5) captures the trend of declining Arctic sea ice extent over the period

of satellite observations. Based on these validation studies, ~~it can be assumed~~ we consider that the CESM1-CAM5-BGC-LE time series is ~~an adequate~~ a fair proxy to study the ~~variability of Arctic sea ice thickness under different conditions. The dataset contains~~ variabilities of the Arctic SIT and SIV under different forcing conditions.

In this paper, we use the monthly averaged Arctic SIT and SIV provided over the 3 ~~main simulations. The first one is a~~ periods (pre-industrial, historical and future). The pre-industrial period is represented by a single 1700-yr control simulation with constant pre-industrial forcing. The ocean model was initialised from a state of rest (Danabasoglu *et al.*, 2012), while the atmosphere, land and sea ice models were initialised using previous CESM1(CAM5) simulations. This experimental design allows the assessment of internal climate variability in the absence of climate change. ~~The two other simulations are a historical (~~In practical terms, we will use the last 200 years of this simulation. The historical period has one ensemble member covering the 1850-2005 ~~) simulation and a future climate simulation~~ period and 30 ensemble members over 1920-2005. Also with 30 ensemble members, the future climate period (2006-2100) ~~following~~ follows the representative concentration pathway (RCP) 8.5 scenario, corresponding to a total radiative forcing of 8.5 W/m^2 in 2100 relative to pre-industrial conditions (Meinshausen *et al.*, 2011). The Canadian Archipelago region was removed from the dataset ~~due to sea ice thickness reaching~~ since SIT reaches unrealistic values in this area.

~~In this paper, we use the monthly averaged Arctic sea ice thicknesses (SIT) provided over the 3 periods (pre-industrial, historical and future). The variability analysisis applied on the SIT and sea ice volume (SIV) anomaly time series. The~~ For the variability analysis, the trend and seasonal cycle are removed ~~to focus on the long-term variability. The anomaly is calculated in three steps. For each month, we build a time series with all values of that month over the entire period. Then, we compute the second degree polynomial fitting the time series. Finally, we remove that polynomial fitting from the original time series. Repeating those steps for each month, we get the original time series without the trend and seasonal cycle.~~ from the time series (pan-Arctic SIV and gridded SIT) so that we focus on the interannual variability. Since the spatial variability analysis uses 30 ensemble members, the SIT anomaly fields are computed by removing the ensemble mean to each member. When only one ensemble member is used, as for the temporal analysis, the anomaly is calculated by excluding the individual trend (provided by a second-order polynomial fit) of each month.

2.2 Variability analysis

~~In order to~~ To characterise the internal variability of the Arctic ~~SIT~~sea ice, we aim at inspecting how ~~it evolves over time and whether there are regions marked by different variabilities. Usual spectral analyses assume stationary of the time series. Having no certainty about the stationary character of the SIV time series even over long periods, we performed the analysis of the temporal variability of the SIV time series by means of wavelet analysis~~the SIV variability evolves in time and how SIT variability is characterized in space. For addressing the temporal variability, we make use of wavelet analysis, with Morlet as wavelet mother, following the methodology proposed by Torrence and Compo (1998). The wavelet analysis ~~is appropriate for~~

non-stationary time series. It determines the evolution of periodicities in the time-space and provides higher resolution in the periodicity (Soon et al. 2011). The wavelet analysis is applied to the SIV anomaly time seriesunder pre-industrial (200-years), has the advantage of taking into account possible non-stationarity of the time series. In this paper, we show the results for one of the historical (1850-2005) and members and one of the future (2006-2100) conditions. members, although we tested the robustness of the results over the 30 ensemble members as discussed later (Section 3.1 and 3.2).

The spatial variability is analysed by computing the EOFs on the SIT anomaly time seriesas conducted by Lindsay and Zhang (2006). This decomposition reduces the large number of variables of the original data to a few variables, but without compromising much of the explained variance. Each EOF represents a mode of SIT variability that provides a simplified representation of the state of the SIT at that time along that EOF. In other words, the EOFs themselves are fixed in time but their weighting coefficients are time-varying; the associated time series (one for each mode) indicate in which state the SIT is at any time (Hannachi, 2004). The analysis is made on the gridded SIT anomaly time series , over the same periodsas defined for the temporal analysis, except for the future climate period which spans from 2006 to 2050 (reasons are given in Section 3.1for the 3 periods. For the historical and future periods, the EOFs are computed over 30 ensemble members, all appended together over time (as done by Labe *et al.*, 2018).

By applying the analysis those analyses separately over the 3 periods we aim to document the internal variability in the absence of any external forcing during the pre-industrial periodand estimate the evolution of the SIT internal variability under anthropogenic forcing, by . By comparing the pre-industrial results with those for the historical and future periods, we estimate the evolution of the SIT and SIV internal variability under anthropogenic forcing.

3 Results

3.1 Temporal variability

The results from the wavelet analysis are presented in Figure 1a-c, in which the global wavelet wavelet power spectrum is shown as a function of time (bottom-left of each subfigure). The time-integrated On the wavelet power spectrum, the crosshatched area denotes the "cone of influence", in which edge effects become important, and the red lines denote the 95% significance levels above a red noise background spectrum. The global wavelet spectrum is also shown (bottom-right), which is a time-integrated power of the global wavelet wavelet power spectrum. The significance level of the time-integrated wavelet spectrum is indicated by the dashed curve; it . It refers to the power of the red noise level at the 95% confidence level that increases with decreasing frequency.

The temporal variability of the Arctic SIV anomaly over the pre-industrial period is depicted in Figure 1a. The time-integrated power spectrum (bottom-right) shows 2 peaks of significant variability. The first peak corresponds to a period centered on 8 years but spanning from 5 to 10 years. The second one corresponds to a period of 16 years spanning from 10 to 20 years.

~~Another peak, presenting a periodicity of 42 years, is present but not taken into account since the peak is below the significance level. The~~ In the wavelet power spectrum~~is presented in the bottom-left panel of Figure 1a,~~, the red lines enclose regions in which the ~~significant variability is highlighted by the regions enclosed by the yellow line. Two first~~ variability is significant. The two main peaks are present throughout the ~~period, but they do not appear together at the same time~~time span, but not always concomitantly. Depending on the time, ~~either~~ both the 8- ~~or 16-years peak is the dominant peak~~and 16-year periods are significant with one of them appearing stronger in the power spectrum (Figure 1a, bottom-left panel). For instance, the ~~8-years~~ 8-year peak is dominant during the 1780-1810 ~~and 1825-1840 periods, and the 16-years~~ period, the 16-year peak during the ~~1750-1790 and~~ 1750-1780 period, and both peaks are dominant during the 1830-1850 ~~periods~~period.

Over the historical period, the Arctic SIV temporal variability shows a first peak centered on 5 years and two others centered on 10 and 16 years, all with 95% ~~reliability. Regarding the~~ confidence (Figure 1b). The wavelet power spectrum ~~, it exhibits a constant line of variability at 16 years and another one, but less constant over the whole period , at 8 years. Those peaks and bands of variability are shown in Figure 1b.~~shows that the 16-year period is significant throughout the entire time span, while the 8-year period loses significance around certain periods of time (e.g., around 1925). The future climate SIV wavelet analysis in Figure 1c presents a clear loss of variability after the year 2050. This loss of variability is visible in the SIV time series and is confirmed by both the wavelet power spectrum and the time-integrated power spectrum. The 2050 sudden loss of variability coincides with the ice-free summer events occurring at that time. Apart from that loss of variability, the wavelet power spectrum exhibits one band of 5-years variability during the ~~2010-2025~~ 2015-2025 period and another band of ~~16-years~~ 10-years variability during the 2025-2050 period, both bands with 95% of confidence. In Figure 1c, the peaks are not significant on the time-integrated power spectrum because the respective variability is significant only over the the first 50 years as it is shown in the wavelet power spectrum (areas in red).

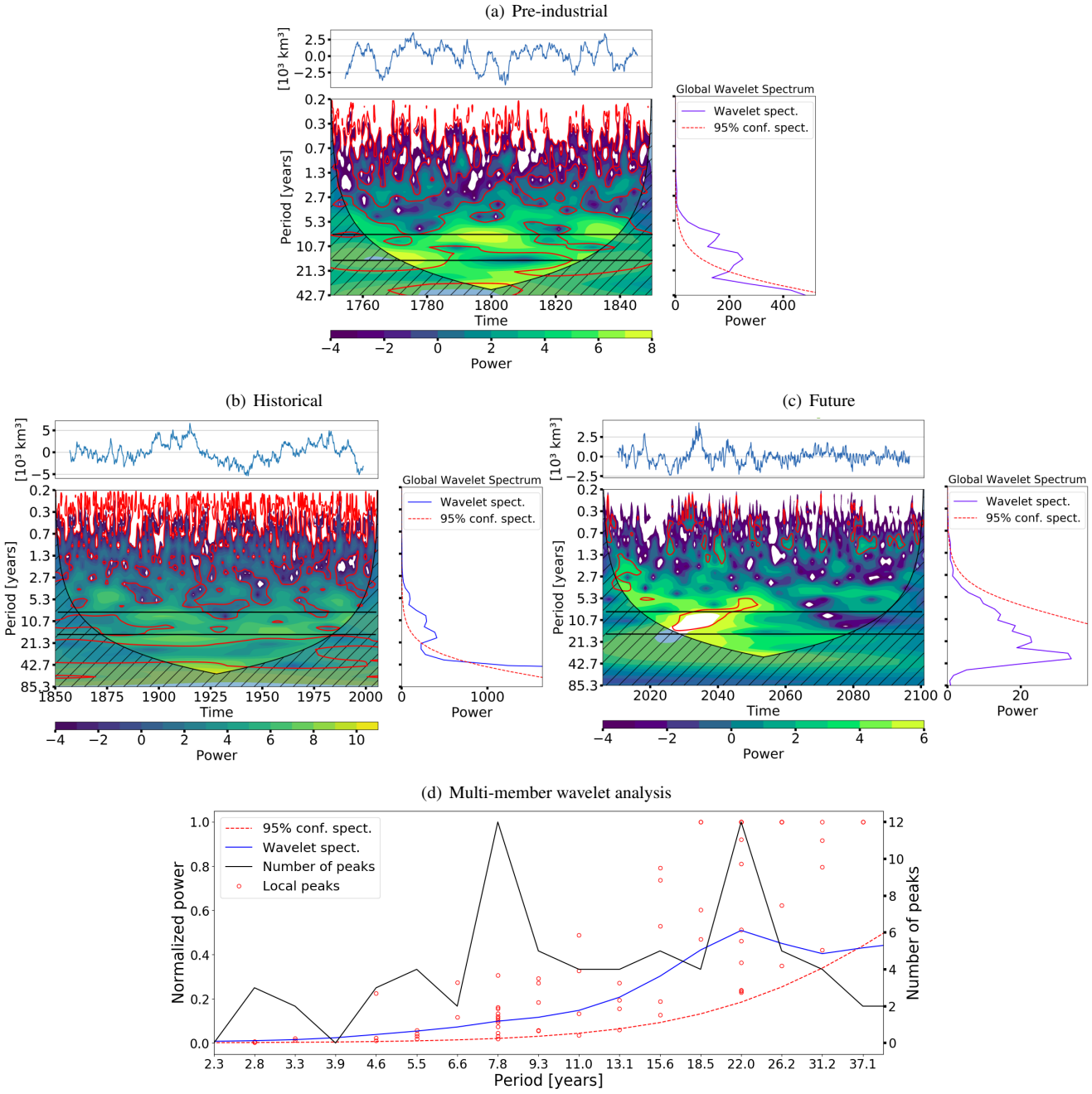

Figure 1. Wavelet analysis ~~, with Morlet as the mother wavelet,~~ applied to the Arctic sea ice volume anomaly over the pre-industrial (200 years preceding the historical integration) (a), historical (1850-2005) (b) and future (2006-2100) (c) periods. Each ~~of the~~ subfigure (a-c) presents the sea ice volume anomaly time series (top), ~~the~~ wavelet power spectrum (bottom-left), and ~~the~~ time-integrated power spectrum from the wavelet analysis (bottom-right). Morlet is used as a wavelet mother. The red lines denote the 95% significance levels above a red noise background spectrum, while the crosshatched areas indicate the cone of influence where edge effects become important. White areas in the wavelet power spectrum are representing values out of the range defined by the color bar. Horizontal black lines depict the 8 and 16-year periods. Multi-members wavelet analysis (d). The red dots depict wavelet spectrum local maxima for all members. The blue and dashed red lines show the mean normalised wavelet spectrum and 95% confidence spectrum for all members, respectively. The black line represent the number of wavelet spectrum local maxima at each period.

The main characteristics of the temporal variability of the Arctic SIV under pre-industrial conditions ~~seems~~ seem to persist under ~~anthopogenic~~ anthropogenic forcing. The two ~~main~~ major temporal peaks of variability centered on 8 ~~years~~ and 16 years, found in the pre-industrial run, are ~~present as band of variability in the power spectrum or peak of variability in the wavelet spectrum in both the historical periodand~~ also present during the historical period. For the first half of the 21st century~~.~~, the future projections are also dominated by the two main peaks but centered at 5 and 10 years in the integrated spectrum, and with relatively weaker power compared to the pre-industrial and historical runs. Furthermore, the SIV variability seems to be non-stationary ~~. Indeed, for a certain period, the main periodicity of the SIV variability can be either centered on 8 or 16 years.~~since the power is not always above the 95% significance level.

The wavelet analyses applied to the other 30 ensemble members of the historical and future simulations bring robustness to our results since, overall, each member shows a similar pattern of temporal variability. To promote such a multi-member comparison among the different spectra, we have first normalised all spectra (and the significance curve) by their respective maximum value so that the power ranges from 0 and 1. This step is required to make that the spectrum from each member has the same weight in the averaging. As shown in Figure 1d (blue line), the averaged spectrum is smoothed out across the time domain because the peaks from different spectra are not co-located exactly at the same periods. Nevertheless, it is still showing that the variability is significant over the background red noise (see dashed red line). To complement this analysis, we have counted the number of local peaks for each period and from all 30 spectra. As shown by the black line in Figure1d, there is a concentration of peaks around the 8-year and 22-year periods. This spread compared to the reference historical run is somehow expected since the internal variability between the different members is not expected to be identical, and even tends to increase with time (Blanchard-Wrigglesworth *et al.*, 2011). For members covering the 21st century, the results are close to the one-member analysis discussed above.

3.2 Spatial variability

The spatial variability of the Arctic SIT anomaly is depicted by the major modes of variability in Figure 2. Since the SIV exhibits a strong loss of variability around the year 2050, the future period for this spatial variability analysis spans from 2006 to 2050. For each period, the modes are sorted by percentage of variability explained. The first mode, which explains most of the variability, represents 22, ~~19~~ 20 and 20 % of the variability for pre-industrial, historical and future climate conditions, respectively. All periods show the same pattern of SIT spatial variability for the first mode. It corresponds to a dipole between the Fram Strait area and the East Siberian Sea (Figure 2 (a,b,c)). For both the pre-industrial and historical periods, the second mode of variability is a pole centered in the East Siberian Sea~~and~~ , but also spreading into the Arctic Basin (Figure 2 (d,e)). It accounts for 14 and ~~17~~ 11 % of the variability, respectively. The third mode of variability for the pre-industrial period corresponds to a dipole between the Laptev and Kara Seas, on the one hand, and the east coast of Greenland, the Chukchi ~~and Beaufort Seas~~ sea and Beaufort Sea, on the other hand.

The first mode of SIT is stable over time and stays the dominant mode of spatial variability in all three periods. ~~The~~ There are some disparities in percentage explained and in magnitude~~are few and some of them can be related to the length of the time series~~, which could be explained by the different lengths of the periods. As the first mode, the second mode of SIT spatial variability is persistent in ~~both the pre-industrial and historical periods, but not in~~ the historical period. For the future climate period~~. Indeed~~, the second mode of SIT variability ~~under future climate conditions presents a pole of variability centered in the Arctic Basin, but regions of highest variability are close to the Canadian Archipelago and not~~ is no longer persistent. It presents a dipole of variability as the first mode, but the Pacific part of the dipole is larger and no longer located in the East Siberian Sea~~, as it is the case for the second mode of the pre-industrial and historical periods~~. The third modes of the three periods (Figure 2 (g,h,i)) exhibit all different patterns of variability and ~~we are not going to use them in the following~~ they are not considered in further analysis.

After 2050, the SIT spatial variability is impacted by the sudden decrease in SIT. EOFs computed over the 2050-2100 period (not shown) exhibit the same pattern of the dipole as the first mode for the 2005-2050 period, but the area of high variability is not the same. The Atlantic part of the dipole is shifted toward the north coast of Greenland and the Pacific part of the dipole is also reduced near the coast.

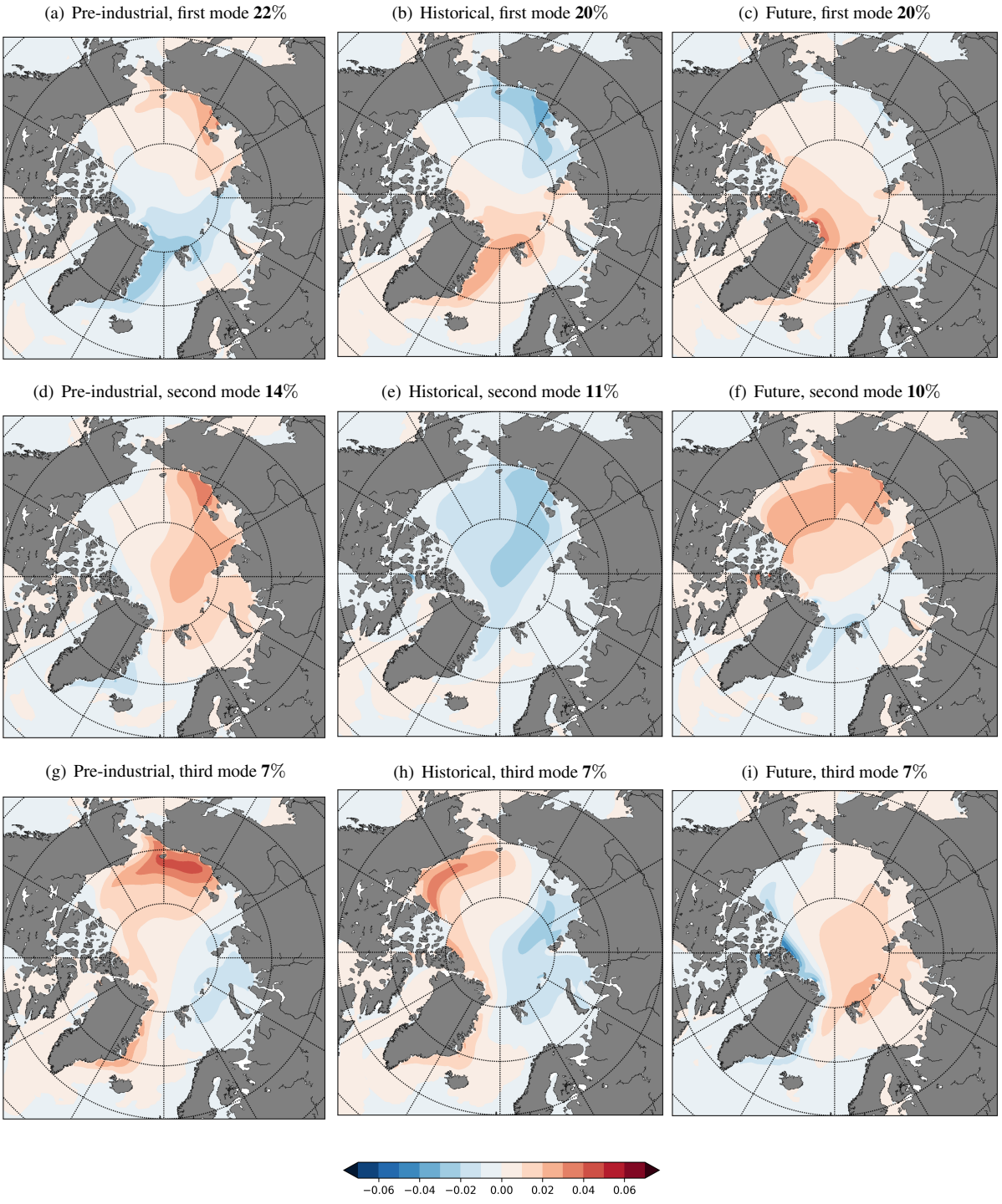

Figure 2. Modes of Arctic SIT spatial variability. From the left to the right, each row shows the three first EOF of Arctic SIT over the pre-industrial (200 years preceding the historical integration) (a,d,g), historical (1920-2005) (b,e,h) and future (2006-2050) (c,f,i) periods, respectively. EOFs for the historical and future periods are performed over 30 ensemble members.

3.3 Drivers of the major modes of SIT internal variability

By computing the temporal oscillation between phases of a certain mode of variability, we are able to characterise this mode by low and high indices. In order to find the physical drivers of the SIT modes of variability, we investigate the differences in dynamic and thermodynamic features (sea ice velocity, atmospheric surface temperature) between both phases of the modes. ~~We looked at the mean sea ice circulation for each phase. Figure 3shows the Arctic mean~~ Figure 3a,b show the mean Arctic sea ice circulation over the pre-industrial period by compositing the low (a) and high (b) indices for the first mode of SIT variability. The sea ice drift anomaly associated with the positive and negative phases of the first SIT mode share similar features with the Arctic Oscillation: a cyclonic anomaly in the Beaufort Gyre, impacting the Transpolar Drift Stream, the Laptev Sea Gyre and the East Siberian circulation, as described by Rigor *et al*., (2002).

Furthermore, applying wavelet analysis to the associated time series of the first spatial mode of variability indicates that the main periodicity of this mode is centered on 8 years and spans from 5 to 10 years (not shown). This result ~~allows us to link~~ is suggestive of a link between the first mode of temporal variability of the wavelet analysis ~~to~~ and the first mode of spatial variability, and so, to the Arctic Oscillation.

We also used the associated time series of the second mode of SIT spatial variability to characterise it by low and high indices. The same analysis over the sea ice velocity is performed for the second mode. For both indices, the sea ice velocity fields are similar. We concluded that the second mode is not dynamically driven. Following Olonscheck *et al*. (2019) results, which demonstrate that the internal variability of Arctic sea ice area and concentration are primarily caused by atmospheric temperature fluctuations, we investigated the differences in mean surface air temperature anomaly over the pre-industrial period between the low ~~(a) and high (b) indices of the second mode~~ and high indices for both the first and second modes of SIT variability~~(see Figure 3)~~. Two widely different states of surface air temperature are found ~~. When the index of the mode of variability is low, the~~ between indices for both modes (the surface air temperature ~~is about 8°C lower than on average over the eastern side of the Arctic Basin. When the index is high,~~anomaly for the second mode is depicted in Figure 3c,d). It appears that the SIT variability and the ~~center and western side of the Arctic Basin are on average colder by 8°C. Those strong discrepancies in mean~~ surface air temperature ~~, characterised by a cooling in the East Siberian, Laptev and Kara Seas in low phase or a cooling in the center and the western side of the Arctic Basin, are then causing strong variability in the SIT over the Arctic Basin through enhanced thermodynamic ice growth.~~are associated with each other.

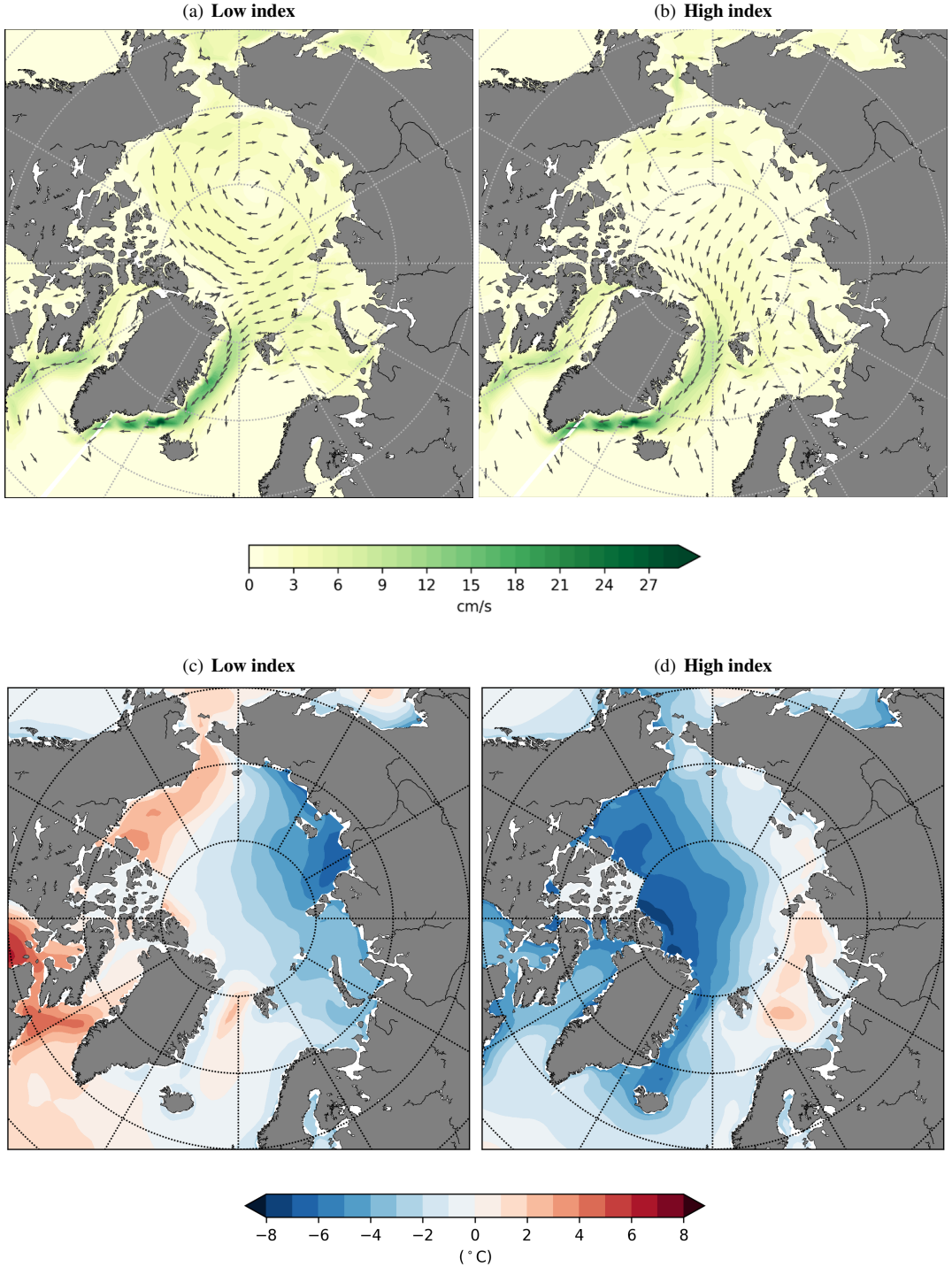

Figure 3. Arctic sea ice mean circulation during low (a) and high (b) indices of the first mode of SIT variability during the pre-industrial period. Arctic mean surface air temperature anomaly during low (c) and high (d) indices of the second mode of SIT variability.

4 Conclusions

In this work, we have analysed the internal variability of the Arctic SIT both spatially and temporally with the CESM1-CAM5-BGC-LE dataset. We conducted ~~a~~ wavelet analysis of the pan-Arctic SIV anomaly and ~~an~~ EOF decomposition of the gridded SIT anomaly, both over a 200-yr control run conducted under pre-industrial conditions. Then, to assess the persistence of the SIT anomaly internal variability under anthropogenic forcing, we performed the same analyses ~~over the 1850-2005 historical period and the future (2006-2050 for EOF and 2006-2100 for the wavelet analysis)~~with 30 ensemble members over the historical and future periods.

The temporal analysis of the SIV anomaly internal variability shows ~~2~~ two peaks of significant variability. One centered on 8 years, spanning from 5 to 10 years, and another one centered on 16 years, spanning from 10 to 20 years. These two peaks of temporal variability are present in both the pre-industrial and historical periods, as well as in the first half of the 21 century. After that, a sudden loss of variability due to ice-free summer events is found. Furthermore, despite a dominant periodicity over the three periods, the SIV anomaly has been observed to be non-stationary. Indeed, the dominant periodicity of the SIV variability can be either centered on 8 or 16 years, depending on the timescale and period. Wavelet analyses over the 30 ensemble members for the post-industrial period have shown the same behaviour of temporal variability within members, except that the peaks are not always centered in 8 and 16 years but somewhere between 5-10 and 15-26 years, depending on the member.

The spatial analysis of the SIT anomaly internal variability has been applied to the 30 ensemble members and reveals two important modes of variability. The first one is a mode with opposite signs centered in the East Siberian Sea and in the Fram Strait area, accounting for 22% of the variability in the pre-industrial period. This first mode is a dynamical one, related to the Arctic Oscillation, and persists over all pre-industrial, historical and future periods. Furthermore, this first mode of spatial variability has a temporal variability of 8 years (spanning from 5 to 10 years), corresponding to the first peak of variability found in the temporal analysis. The second mode exhibits a large pole of variation centered on the East Siberian Sea going through the Arctic Basin. It represents 14% of the variability in the pre-industrial period. ~~It is a thermodynamic mode, which is linked to a variation in surface air temperature. This second mode of spatial variability is present in both the pre-industrial and historical periods.~~

The loss of sea ice in summer starting in 2050 and the strong decrease in SIV ~~going from 15 to 10×10^3 km^3~~ in winter during the second half of the 21st century ~~modifies strongly~~ (from 15 to 10×10^3 km^3) strongly modifies the variability of the ice both spatially and temporally. The main modes of spatial variability lose their significance or just disappear after 2050, and the temporal analysis shows a total disappearance of the variability at that time.

This analysis of the Arctic SIT and SIV variability bears some limits. Indeed, our results for the temporal and spatial patterns of variability are based on only one model, and despite the use of 30 ensemble members and a reasonable validation against

observations, the model is not perfect. Furthermore, the spatial modes of SIT variability are robust for all the 30 ensemble members but the temporal analysis shows some dissimilarities between members. Other studies with other model outputs are therefore needed to confirm our conclusion.

Finally, in the context of recent climate changes, predicting sea ice has never been so important. ~~Therefore, our analysis of the Arctic SIT and SIV internal variability could lead to better mooring and observing devices, able to improve our day-to-day observation of Arctic sea ice thickness andvolume data, which~~ However, to validate and improve our predictions, observational data is crucial. In this sense, our variability analysis of internal SIV and SIT variability might help the development of an optimal sampling strategy, taking into account the selection of well-placed sampling locations for monitoring the SIT and, therefore, the pan-Arctic SIV, that are not as well documented as the sea ice extent ~~or sea ice area .~~ and area (Ponsoni *et al.*, 2019).

Data availability. Data can be downloaded from the following source: https://www.earthsystemgrid.org/dataset/ucar.cgd.ccsm4.CESM_CAM5_BGC_LE.ice.proc.monthly_ave.html. The 30 ensemble members used in this study are the first 30 members (001-030).

Code and data availability. The wavelet analysis is performed with the Waipy module on Python. https://github.com/mabelcalim/waipy

Competing interests. The authors declare that they have no conflict of interest.

Acknowledgements. The work presented in this paper has received funding from the European Union's Horizon 2020 Research and Innovation programme under grant agreement no. 727862: APPLICATE project (Advanced prediction in Polar regions and beyond). We also thank the EU Horizon 2020 PRIMAVERA project, grant agreement no. 641727. François Massonnet and Leandro Ponsoni are F.R.S.-FNRS ~~PostDoc and Research Associate~~ Research Associate and Post Dotoral Researcher, respectively. Guillian Van Achter is founded by PARAMOUR project which is supported by the Excellence Of Science programme (EOS), also founded by FNRS. We thank the two referees for their very helpful comments on a earlier version of this manuscript. The dataset used in this study was made available by CESM Community.

References

Barnhart, K. R., Miller, C. M., Overeem, I., and Kay, E.:Mapping the future expansion of Arctic open water, Nature Clim Change, 6, 280–285, doi: 10.1038/NCLIMATE2848, 2016.

Blanchard-Wrigglesworth, E., Bitz, C. M., and Holland, M. M.:Influence of Initial Conditions and Climate Forcing on Predicting Arctic Sea Ice. Geophysical Research Letters 38, no 18, https://doi.org/10.1029/2011GL048807, 2011.

Deser, C., Philips, A. S., Alexander, M. A., and Smoliak, B. V.:Projecting North American Climate over the Next 50 Years: Uncertainty due to Internal Variability, Journal of Climate, 27, 2271-2296, doi.org/10.1175/JCLI-D-13-00451.1, 2014.

Deser, C., Philips, A., Bourdette, V., and Teng, H.:Uncertainty in climate change projections: the role of internal variability, Climate Dynamics, 38, 527–546, doi.org/10.1007/s00382-010-0977-x, 2012.

Fučkar, N. S., Guemas, V., Johnson, N. C., Massonnet, F., and Doblas-Reyes, F.: Clusters of Interannual Sea Ice Variability in the Northern Hemisphere, Climate Dynamics, 47, 1527–1543, doi.org/10.1007/s00382-015-2917-2, 2016.

Hannachi, A.:A Primer for EOF Analysis of Climate Data, Department of Meteorology, University of Reading Reading, 2004.

Jahn, A., Kay, J. E., Holland, M. M., and Hall, D. M.:How predictable is the timing of a summer ice-free Arctic?, Geophys. Res.Lett., 43, 9113–9120, doi:10.1002/2016GL070067, 2016.

Kay, J.E., Deser, C., Phillips, A., Mai, A., Hannay, C., Strand, G., Arblaster, J.M., Bates, S.C., Danabasasoglu, D., Edwards, J., Holland, M., Kushner, P., Lamarque, J.-F., Lawrence, D. , Lindsay, K., Midd Leton, A., Munoz, E., Neale, E., Oleson, K., Polvani, L., and Vertenstein, M.:The Community Earth System Model (CESM) Large Ensemble Project, A Community Resource for Studying Climate Change in the Presence of Internal Climate Variability, American Meteorological society, 1333-1349, doi.org/10.1175/BAMS-D-13-00255.1, 2015.

Kwok, R.:Arctic sea ice thickness, volume, and multiyear ice coverage: losses and coupled variability (1958–2018), Environ. Res. Lett., 13, 10, https://doi.org/10.1088/1748-9326/aae3ec, 2018.

Labe, Z., Magnusdottir, G., and Stern, H.:Variability of Arctic Sea Ice Thickness Using PIOMAS and the CESM Large Ensemble. J. Climate, 31, 3233–3247, https://doi.org/10.1175/JCLI-D-17-0436.1, 2018.

Lindsay, K., Bonan, G. B., Doney, S. C., Hoffman, F. M., Lawrence, D. M., Long, M. C., Mahowald, N. M., Moore, J. K., Randerson, J. T., and Thornton, P. E.:Preindustrial-control and twentieth-century carbon cycle experiments with the Earth system model CESM1(BGC), J. Climate, 27, 8981-9005, doi.org/10.1175/JCLI-D-12-00565.1, 2014.

Lindsay, R. W., and Zhang, J.: Arctic Ocean Ice Thickness: Modes of variability and the Best Locations from Which to Monitor Them, Journal of physical oceanography, 36, 496-506, doi.org/10.1175/JPO2861.1, 2006.

Meinshausen, M., Calvin, S. J., Daniel, J. S., Kainuma, M. L. T., Lamarque, J-F., Matsumoto, K., and Montzka, S. A.:The RCP greenhouse gas concentrations and their extensions from 1765 to 2300, Climatic Change, 109-213, doi.org/10.1007/s10584-011-0156-z, 2011.

Moore, C. P., Lindsay, K., Doney, S. C., Long, S. C., and Misumi, K.:Marine ecosystem dynamics and biogeochemical cycling in the Community Earth System Model[CESM1(BGC)]:Comparison of the 1990s with the 2090s under the RCP4.5 and RCP8.5 scenarios, J. Climate, 26, 9291-9312, doi.org/10.1029/2011JD017187, 2013.

Notz, D., and Stroeve, J.:Observed Arctic sea-ice loss directly follows anthropogenic CO2 emission, Science, 354, 747-750, doi: 10.1126/science.aag2345, 2016.

Olonscheck, D., Mauritsen, T., and Notz, D.: Arctic Sea-Ice Variability Is Primarily Driven by Atmospheric Temperature Fluctuations, Nature Geoscience, 12, 6, 430–34, doi.org/10.1038/s41561-019-0363-1, 2019.

Olonscheck, D., and Notz, D.: Consistently estimating internal climate variability from climate-model simulations, J. Climate, 30, 9555-9573, doi:10.1175/JCLI-D-16-0428.1, 2017.

Onarheim, I. H., Eldevik, T., Smedsrud, L. H., and Stroeve, J. C.: Seasonal and Regional Manifestation of Arctic Sea Ice Loss, J. Climate, 31, 4917–4932, https://doi.org/10.1175/JCLI-D-17-0427.1, 2018.

Ponsoni, L., Massonnet, F., Docquier, D., Van Achter, G., and Fichefet, T.: Statistical predictability of the Arctic sea ice volume anomaly: identifying predictors and optimal sampling locations, The Cryosphere Discuss., https://doi.org/10.5194/tc-2019-257, in review, 2019.

Rigor, I. G., Wallace, J. M., and Colony, R. L.:Response of Sea Ice to the Arctic Oscillation, Journal of Climate, 15, 2648, doi.org/10.1175/1520-0442(2002)015<2648:ROSITT>2.0.CO;2, 2002.

~~Singarayer, J. S., and Bamber, J. L.:EOF analysis of three records of sea-ice concentration spanning the last thirty years, Geophys. Res. Lett, 30, 1251, doi.org/10.1029/2002GL016640, 2003.~~

Soon, W., Dutta, K., Legates, D. R., Velasco, V., and Zhang, W. J.: Variation in surface air temperature of China during the 20th century, Journal of Atmospheric and Solar-Terrestrial Physics, 73, 2331-2344, doi:10.1016/j.jastp.2011.07.007, 2011.

Stroeve, J., Barrett, A., Serreze, M., and Schweiger, A.: Using records from submarine, aircraft and satellites to evaluate climate model simulations of Arctic sea ice thickness, The Cryosphere, 8, 1839-1854, doi.org/10.5194/tc-8-1839-2014, 2014.